RSC Chemical Biology

ROYAL SOCIETY OF CHEMISTRY

COMMUNICATION

View Article Online
View Journal | View Issue



Cite this: *RSC Chem. Biol.*, 2023, 4, 871

Received 29th May 2023,
Accepted 22nd September 2023

DOI: 10.1039/d3cb00079f

rsc.li/rsc-chembio

# Red-shifted activity-based sensors for ethylene *via* direct conjugation of fluorophore to metal–carbene†

Nicholas J. Dacon, Nathan B. Wu and Brian W. Michel *

**A number of Activity-Based Sensors (ABS) for relatively unreactive small molecules, such as ethylene, necessitates a transition metal for reaction under ambient conditions. Olefin metathesis has emerged as one of the primary strategies to achieve ethylene detection, and other transition metals are used for similarly challenging-to-detect analytes. However, limited studies exist investigating how fluorophore-metal attachment impacts photophysical properties of such ABS. Two new probes were prepared with the chelating benzlidene Ru–ligand directly conjugated to a BODIPY fluorophore and the photophysical properties of the new conjugated ABS were evaluated.**



## Introduction

The simplest alkene ethylene (IUPAC name ethene) has a range of important and interesting roles in biological systems. Ethylene is an important plant hormone well-known for its role in the ripening of climacteric fruit, but it also has broad signalling responsibilities affecting the expression of a range of genes.[1–6] Additionally, ethylene is produced in mammalian systems. Peroxidation of unsaturated fatty acids and subsequent radical fragmentation pathways produce ethylene,[7] which can be detected in exhaled breath, making it an intriguing biomarker of oxidative stress.[8]

Molecular detection of ethylene has largely focused on roles in plant systems inspiring several elegant strategies due to the lack of main group reactivity under mild conditions.[9,10] To detect this simple alkene, transition metals have emerged as an obvious choice owing to the wealth of coordination chemistry and reactivity accessible under ambient conditions due to additional bonding interactions such as pi-back bonding.[11] Approaches reported for molecular ethylene detection can be broadly categorized as coordination-based sensors[12–16] or activity-based sensors (ABS)[17–24] with the latter emerging as an attractive approach for selective ethylene detection in complex environments.[9,25,26] In 2018, our group reported a fluorescent tagged Hoveyda–Grubbs-type complex that provided sensitive and selective detection of ethylene (Fig. 1(A)).[18] Since, additional reports have demonstrated olefin metathesis as a viable strategy for ethylene detection along with a recent report using migratory insertion into a cyclorhodinated complex.[23] Beyond ethylene detection, transition metal-based ethylene probes represent examples of transition-metal based ABS, which are gaining traction for the detection of small molecule analytes that lack reactive functionality.[27–35]

To improve sensitivity for ethylene, it is desirable to increase signal response to ethylene while minimizing background

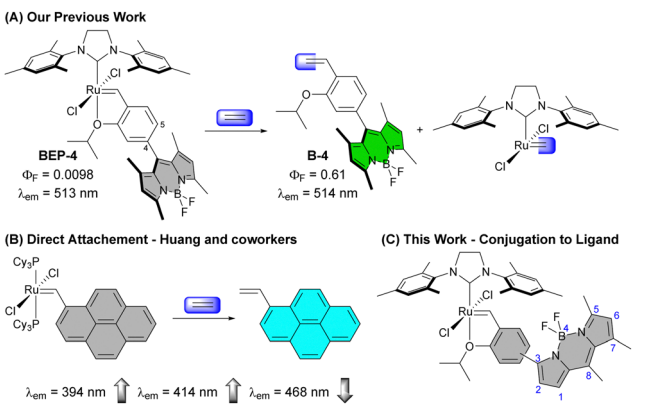


Fig. 1 (A) Previously reported probes **BEP-4** and **BEP-5** (not shown) demonstrated a large (~113-fold) increase in luminescence to ethylene with minimal shift in the wavelength of emission. (B) The Grubbs 1st generation Ru complex derived from 1-vinylpyrene was reported by Huang and coworkers with 20-fold increase in luminescence. (C) The work described here evaluates modified BODIPY ethylene probes with the chelating benzylidene ligand conjugated to the extended fluorophore π system – **Con-BEP**s.

*Department of Chemistry and Biochemistry, University of Denver, Denver, CO, 80210, USA. E-mail: Brian.Michel@du.edu*

† Electronic supplementary information (ESI) available: Additional experimental details, photophysical characterization data, supplemental figures, and NMR spectra. See DOI: https://doi.org/10.1039/d3cb00079f

signal. One effective approach has been to "protect" the ruthenium complex in hydrophobic binding pockets of proteins such as albumin, which is an intriguing strategy with a range of potential applications.[20,22,36] Alternatively, we have been interested in using ligand modulation[37] about the reactive ruthenium species to improve signal and reactivity. More broadly transition metal-based ABS are often quenched prior to analyte detection by the presence of the metal. Therefore, it is important to understand how different means of connecting the reactive ligand to the fluorophore impact the optical properties of the ABS.

A Grubbs 1st generation-based probe reported by Huang and co-workers has the Ru directly bound to a fluorescent pyrene core (Fig. 1(B)).[19] This probe shows an interesting modulation of emission peaks upon reaction with ethylene with a decrease in intensity of a small peak at 468 nm and increase in the peaks at 394 and 414 nm. Other Ru- and Rh-based ethylene probes reported to date show only the expected increase in emission intensity upon reaction with ethylene.

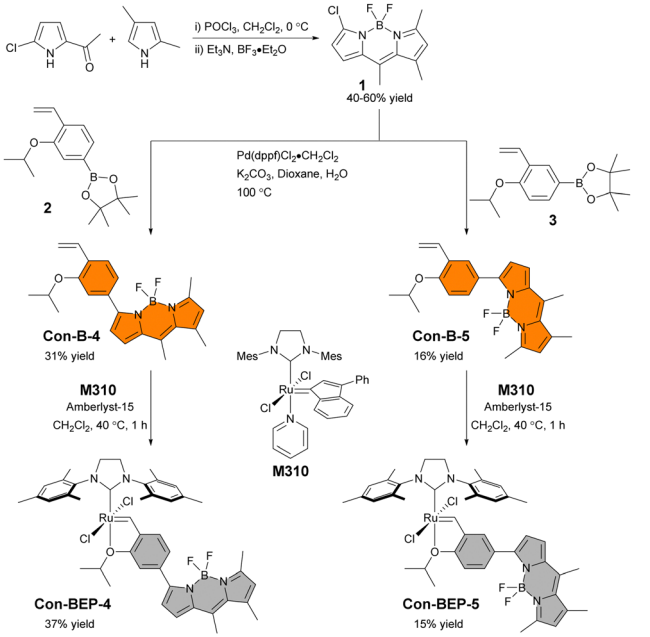


Scheme 1 Synthetic routes to **Con-BEP-4** and Con-BEP-5.

## Results and discussion

### Synthesis of Con-BEP-4 and Con-BEP-5

The substitution pattern on the BODIPY of **BEP-4**, with methyl groups at the **1** and 7 positions, restrict rotation of aryl adjacent π systems. In the context of **BEP-4** (or **BEP-5**, not shown) this suggests that quenching occurs *via* a through space process (*i.e.* PET or FRET). We hypothesized that conjugation of the chelating ligand to the fluorophore would result in a red-shifted probe with potentially interesting modulation of the optical properties and instruct future design of transition metal containing ABS. Herein we report the synthesis and characterization of two new conjugated BEPs (**Con-BEP**s), one of which displays large turn-on coupled with a hypsochromic shift of the emission peak relative to the ethylene adduct.

We initially sought to prepare two complexes with the chelating isopropoxy styrene at the 3-position of the BODIPY analogous to **BEP-4** and **BEP-5**. To achieve this, we envisioned a convergent route (Scheme 1) coupling the known asymmetric chloro-BODIPY **1**[38] and the pinacol boronate esters **2** and **3**, which are readily prepared from the commercially available bromo salicyladehydes. Pd-mediated cross coupling provided the ligands **Con-B-4** and **Con-B-5** in unoptimized 31% and 16% yields, respectively, providing sufficient material for preparing the desired Ru-complexes. **Con-BEP-4** and **Con-BEP-5** were prepared using the indenylidene monopyridine complex (**M310**) and Amberlyst-15 resin.[39,40] In our hands, we have found this to be the most reliable method for preparing high purity complexes. This procedure is touted for operational simplicity and not requiring column chromatography; however, the presence of even a small amount highly fluorescent impurity results in a higher baseline signal and reduced turn-on for ethylene detection. As a result, we have found synthesis and chromatographic purification of the final complex in a nitrogen filled glove box beneficial. This provides isolated complex with the largest observed turn-on, although batch to batch variability was still observed. It should be noted that these complexes are bench stable in the solid state after purification.

### Photophysical characterization and structure

The optical properties of the quenched **Con-BEP**s were investigated along with their respective precursors (Fig. 2(A)). Both Ru complexes, **Con-BEP-5** and **Con-BEP-4**, were efficiently quenched and the corresponding ethylene adducts, **Con-B-5** and **Con-B-4** are strongly emissive. As expected, all four compounds were red shifted as compared to **BEP-4** and the further separation from the primary absorption of **HG2** supports an electron transfer quenching process over an energy transfer (Fig. 2(B)).

**Con-BEP-4** displays some additional noteworthy photophysical features including a hypsochromic shift of the emission peak relative to **Con-B-4**, which is potentially valuable effect that presumably arises from the positioning of the Ru para to the BODIPY. Further, comparison of the absorbance spectrum showed a surprising broadening and bathochromic shift for **Con-BEP-4**, which is not observed for the other three compounds (Fig. 2(C)). This puts the $\lambda_{abs}$ almost on top of the $\lambda_{em}$, yet the excitation spectrum does not overlay the absorption (Fig. 2(D)). This interesting series of observations may explain the more quenched fluorescence observed for **Con-BEP-4** and we suspect it is related to non-emissive absorption arising from extended conjugation to the benzylidene carbon.

Although the red-shifted emission supports extended conjugation of the fluorophore pi-system, we sought additional information on the structural implications of incorporating the aryl unit at the 3-position of the BODIPY. DFT calculations were performed b3lyp/6-311+G(d), which identified an energy minimized structure with a dihedral angle of 38° between the

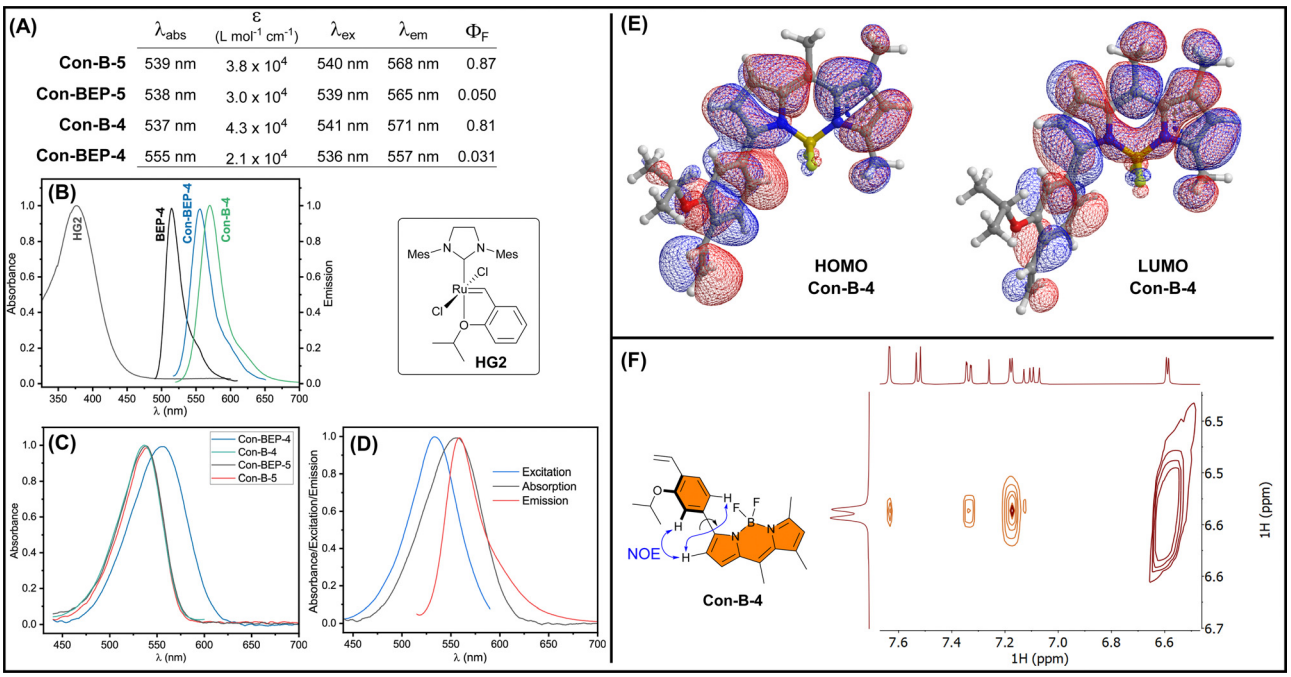


Fig. 2 (A) Summary of the photophysical properties of Con-BEP-5 and **Con-BEP-4** along with the ethylene adducts measured in PhMe at RT. Molar absorptivity ($\varepsilon$) measured at the respective $\lambda_{abs}$ maxima. (B) Comparison of the absorption spectrum of HG2 (gray) with the emission spectra for BEP-4 (black), **Con-BEP-4** (blue), and **Con-B-4** (green) showing minimal spectral overlap. (C) Absorption spectra for the Con-BEPs and ethylene adducts: **Con-B-4**/5. (D) Excitation, absorption, and emission spectra for **Con-BEP-4**. (E) Calculated molecular orbitals for **Con-B-4**. (F) 2D NOESY spectrum for **Con-B-4**.

BODIPY and aryl units (Fig. 2(E)). Forcing a more planar structure with a dihedral angle of 8° results in a 2 kcal mol$^{-1}$ penalty (see ESI†). In both conformations the HOMO (and HOMO−1) for both structures extends across the BODIPY and aryl moieties. To gain insight into the solution structure, a NOESY spectrum of **Con-B-4** was acquired (Fig. 2(F)). Notably, through space correlations were observed between the proximal pyrrole H and both ortho H's of the arene unit suggesting a range of conformations are readily accessible about the BODIPY-aryl bond.

## Response to ethylene

Next, the fluorescence response of **Con-BEP-5** and **Con-BEP-4** to ethylene was evaluated (Fig. 3(A)). **Con-BEP-5** showed an ~15-fold increase in integrated emission over 60 min and an endpoint turn-on of 22-fold (Fig. S14, ESI†). Notably **Con-BEP-4** had a much larger increase in fluorescence upon exposure to excess ethylene along with an ~14 nm bathochromic shift of $\lambda_{em}$ (Fig. 3(B)). Integrating the emission peak showed up to a 123-fold turn-on in 60 min and an endpoint turn-on of 160-fold (Fig. 3(C)). However, by taking advantage of the shift in the emission peak and monitoring turn-on at the wavelengths of maximal difference (~580–581 nm), a 179-fold turn-on was observed in 60 min with an endpoint turn-on of 235-fold!

The kinetic profiles for both probes were measured by adding probe to a saturated solution of ethylene in toluene at 25 °C. The increase in fluorescence intensity was monitored under these pseudo-first-order conditions as a measure of product formation (see ESI† for full details). The observed rate

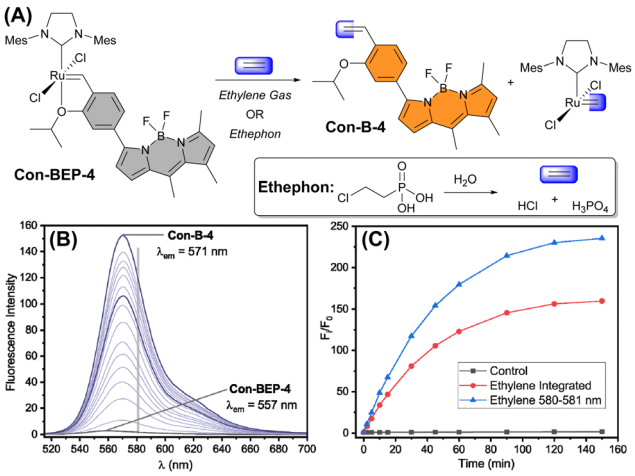


Fig. 3 (A) Reaction of **Con-BEP-4** with ethylene gas or ethylene from ethephon hydrolysis. (B) Emission spectra of **Con-BEP-4** exposed to ethylene. Timepoints represented are $t$ = 0, 5, 10, 15, 20, 25, 30, 40, 50, 60, 75, 90, 105, 120, 150, and 180 min. Gray bar at 581 nm represents wavelength with maximum increase in emission intensity. (C) Normalized emission intensity of **Con-BEP-4** control sample or treated with ethylene (integrated emission and 580–581 nm).

constants ($k_{obs}$) for **Con-BEP-5** ($k_{obs} = 4.1 \times 10^{-4} \pm 0.3$ s$^{-1}$) and **Con-BEP-4** ($k_{obs} = 3.1 \times 10^{-4} \pm 0.3$ s$^{-1}$) were of similar magnitude, which is not surprising given the minimal structural changes to the coordination environment about Ru.

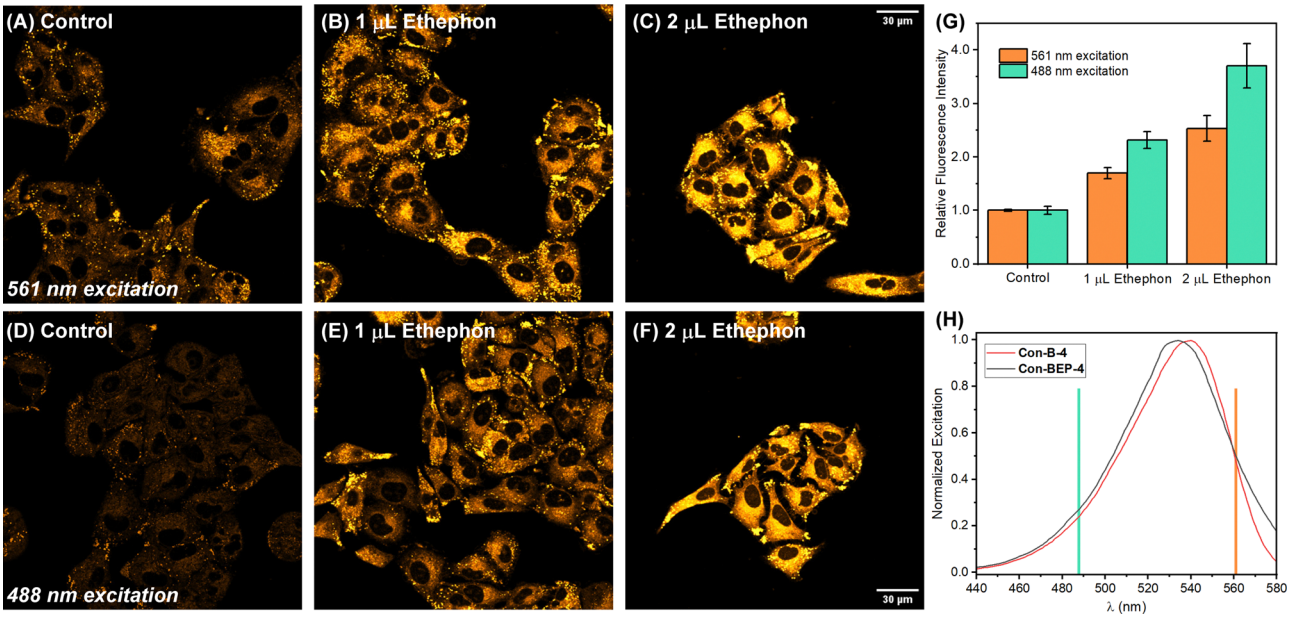


Fig. 4 Representative confocal microscopy images of A549 cells treated with varying amounts of ethephon followed by **Con-BEP-4**. (A)–(F) Cells were pre-treated with 0, 1, or 2 μL of ethephon (40% solution) in 400 μL DMEM for 2 h at 37 °C. Cells were washed with PBS and stained with 1 μM **Con-BEP-4** in PBS (0.5% DMSO) for 1 h at 37 °C. Images acquired exciting with a (A)–(C) 561 nm laser or a (D)–(F) 488 nm laser. (H) Mean fluorescence intensity measured across the entire field. Error bars denote ±SD. Statistical analysis was performed using a two-tailed test and all measurements are statistically significant with respect to the control, varied ethephon concentrations, and excitation with different lasers ($p < 0.01$). (I) Excitation scans of **Con-BEP-4** and the ethylene adduct **Con-B-4** with the respective laser lines indicated.

Since direct application of ethylene gas is often impractical in agricultural settings, ethephon (2-chlorophosphonic acid) is used widely to expose plants to a controlled release of ethylene. Due to limited aqueous solubility, similar challenges are presented in accurately dosing ethylene in laboratory settings such as the cell studies described below. Therefore, we sought to demonstrate that ethylene released from slow hydrolysis of ethephon could be detected. **Con-BEP-4** was converted to **Con-B-4** under biphasic conditions (PBS/PhMe), which was readily assessed by NMR (Fig. S18, ESI†). Specifically, the observation of the terminal alkene hydrogens from **Con-B-4** can only be observed from metathesis and not from probe decomposition. In a similar experiment, conversion of **Con-BEP-4** to **Con-B-4** was achieved in the presence of cell growth media (Fig. S19, ESI†).

### Cell studies

Inspired by these intriguing findings **Con-BEP-4** was evaluated for detection of ethylene in live A549 cells. Cells were first treated with varying amounts the ethylene releasing molecule, ethephon, followed by washing, and treating with **Con-BEP-4**. Compared to BEP-4, the red-shifted $\lambda_{ex}$ allows for flexible image acquisition parameters. Images were acquired with two different laser sources and observation windows. Exciting with a 561 nm laser and observing from 578–602 nm showed good turn-on and a dose dependent response to increased concentrations of ethylene (*via* ethephon hydrolysis, Fig. 4(A)–(C) and (G)). Additional images acquired independently with a 488 nm laser source and observing over a wider range of wavelengths, 539–601 nm, showed a larger mean fluorescence response (Fig. 4(D)–(G)). It is possible that the larger response under the later imaging conditions arises from the larger observation window or excitation efficiencies at different wavelengths. However, the later explanation seems unlikely when comparing the laser lines overlayed on the respective excitation spectra of **Con-BEP-4** and **Con-B-4** (Fig. 4(H)). Given that an intermediate laser closer to the excitation maxima was not available, these results highlight the utility of **Con-BEP-4**, and similar fluorophores, for varied experimental and microscope setups.

Finally, the potential for cytotoxicity was evaluated. Cells were exposed to varied concentrations of **Con-BEP-4**, **Con-B-4**, **Con-BEP-5**, and **Con-B-5** under analogues conditions to those used for live-cell imaging. Cell viability was assessed by an MTT assay and no significant toxicity was observed for the concentrations evaluated (Fig. S21, ESI†).

## Conclusions

The direct conjugation of the Hoveyda–Grubbs-type chelating ligand to BODIPY fluorophores at the 3-position results in the expected, red-shifted ethylene probes that may be useful for cellular imaging studies, particularly in mammalian systems. Both **Con-BEP-4** and **Con-BEP-5** are efficiently quenched, despite poor overlap with the absorption peak of HG2. This suggests an electron transfer mechanism as the primary means of quenching and not an energy transfer process. The positioning of the Ru-benzylidene *para* to the BODIPY in **Con-BEP-4** resulted in an interesting hypsochromic shift of ~14 nm relative to ethylene adduct **Con-B-4** and this effect is not

observed for this isomeric **Con-BEP-5**. This shift coupled with the large increase in fluorescence upon reaction with ethylene allows for increased observed turn-on by judicious selection of excitation and observed emission wavelengths. This observation has potential implications in the design of future ethylene probes and more broadly in other transition metal-based ABS. Additionally, imaging studies in live cells demonstrate dose dependent ethylene detection and flexibility in choice of excitation sources treated with varying amounts of ethephon followed by **Con-BEP-4**.

## Materials and methods

### Synthesis of Con-BEP-4 and Con-BEP-5

All reactions utilizing air- or moisture-sensitive reagents were performed in dried glassware under an atmosphere of dry $N_2$. When dry solvent was used the solvent was passed over activated alumina. Other reagents were purchased and used without further purification unless otherwise stated. Silica gel (RediSep Rf gold) was used for column chromatography. Grubbs second generation catalyst, ethylene gas, and all other reagents were purchased from commercial sources and used as received. $^1$H and $^{13}$C NMR spectra for characterization of new compounds were collected in $CDCl_3$ at 25 °C at the NMR Facility at the University of Denver using a Bruker Avance III 500 MHz instrument. All chemical shifts are reported in parts per million and referenced to the residual solvent peak from $CDCl_3$ ($\delta$ = 7.26 ppm, $^1$H; 77.16 ppm, $^{13}$C). Splitting patterns are indicated as follows: s, singlet; d, doublet; t, triplet; dd, doublet of doublets. Glovebox experiments were conducted in a nitrogen-filled glovebox at less than 10 ppm $O_2$ level and 1 ppm $H_2O$. High-Resolution Mass spectrometry data were obtained using a Shimadzu LCMS-9030 Quadrupole iRef TOF in the indicated ionization mode (ESI or APCI).

**2-(3-Isopropoxy-4-vinylphenol)-4,4,5,5-tetramethyl-1,3,2-dioxaborolane (2).** 4-Bromo-2-isopropoxy-1-vinylbenzene (980 mg, 4.06 mmol), KOAc (1.197 g, 12.2 mmol, 3.0 equiv.), Bis(pinacolato) diboron (1.290 g, 5.08 mmol, 1.25 equiv.), and Pd(dppf)$Cl_2$·$CH_2Cl_2$ (166 mg, 0.203 mmol, 0.05 equiv.) were combined in an oven-dried 100 mL 2-neck flask with a magnetic stir-bar and dissolved in 1,4-dioxane (25 mL). The solution was degassed for 20 minutes, and the flask was added to a 75 °C preheated oil bath to stir for 48 hours. After completion, the flask was cooled to room temperature and filtered through a plug of Celite with hexanes and concentrated onto silica. Purified by flash chromatography with hexanes/ethyl acetate to afford the desired product **2** as a white solid (143.5 mg, 0.498 mmol, 12%). $^1$H NMR (500 MHz, $CDCl_3$): $\delta$ 7.49 (d, $J$ = 7.6 Hz, 1H), 7.36 (d, $J$ = 7.6 Hz, 1H), 7.31 (s, 1H), 7.09 (dd, $J$ = 17.8, 11.2 Hz, 1H), 5.78 (dd, $J$ = 17.8, 1.6 Hz, 1H), 5.27 (dd, $J$ = 11.1, 1.6 Hz, 1H), 4.65 (sept, $J$ = 6.1 Hz, 1H), 1.35 (m, 18H – note: the doublet of the isopropyl group and the singlet of the pinacol borate ester overlap). $^{13}$C NMR (126 MHz, $CDCl_3$): $\delta$ 154.8, 132.1, 131.0, 127.3, 125.9, 120.3, 115.0, 83.8, 71.0, 25.0, 22.4. HRMS (APCI$^+$) $m/z$: calculated for $C_{17}H_{26}BO_3$ (M + H$^+$) 289.19695; found 289.19487.

**Con-B-4.** To a 250 mL 2-neck round bottom flask containing **1** (147.7 mg, 0.550 mmol, 1.1 equiv.), **2** (144.1 mg, 0.500 mmol), $K_2CO_3$ (207.3 mg, 1.5 mmol, 3 equiv.) and Pd(dppf)$Cl_2$·$CH_2Cl_2$ (122.5 mg, 0.150 mmol, 0.3 equiv.). A nitrogen atmosphere was established and 1,4-dioxane/water (5 : 1) solution was added to the flask *via* syringe and the solution was degassed for 20 minutes. The flask was added to a 100 °C pre-heated oil bath and stirred for 4.5 hours until completion. The solution was extracted with ethyl acetate (3 × 50 mL) and washed with water and brine (3 × 100 mL), dried with sodium sulfate, and concentrated. Purification by flash chromatography with hexanes/$CH_2Cl_2$ gradient of 40% → 70% to yield **Con-B-4** as an orange solid (61.9 mg, 0.157 mmol, 31%). $^1$H NMR (500 MHz, $CDCl_3$): $\delta$ 7.61 (s, 1H), 7.52 (d, $J$ = 8.2 Hz, 1H), 7.33 (d, $J$ = 8.0 Hz, 1H), 7.19 (d, $J$ = 4.2 Hz, 1H), 7.09 (dd, $J$ = 17.8, 11.2 Hz, 1H), 6.59 (d, $J$ = 4.2 Hz, 1H), 6.14 (s, 1H), 5.80 (d, $J$ = 17.8 Hz, 1H), 5.27 (d, $J$ = 11.2 Hz, 1H), 4.68 (sept, $J$ = 6.2 Hz, 1H), 2.59 (s, 3H), 2.53 (s, 3H), 2.43 (s, 3H), 1.40 (d, $J$ = 6.0 Hz, 6H). $^{13}$C NMR (126 MHz, $CDCl_3$): $\delta$ 158.6, 154.9, 154.4, 143.8, 140.7, 136.3, 133.5, 131.9, 128.1, 126.2, 125.1, 122.7, 121.4 (t, $J_{CF}$ = 2.7 Hz), 118.07, 118.05, 114.9 (t, $J_{CF}$ = 6.1 Hz), 114.6, 70.8, 22.3, 16.9, 16.5, 15.0. HRMS (APCI$^+$) $m/z$: calculated for $C_{23}H_{26}BF_2N_2O$ (M + H$^+$) 395.21008; found 395.20529, $C_{23}H_{25}BF_2N_2ONa$ (M + Na$^+$) 417.19202; found 417.18717.

**Con-BEP-4.** In a $N_2$ filled glovebox, an oven-dried 20 mL Schlenk flask containing **Con-B-4** (28.2 mg, 71.5 μmol), Grubbs Catalyst M310 (53.6 mg, 71.5 μM, 1 equiv.), and amberlyst-15 resin (60.8 mg, 286.1 μM, 4 equiv.) was suspended in anhydrous $CH_2Cl_2$ (2.5 mL). The flask was placed into a 40 °C preheated oil bath to stir for 1 hour after which time the flask was cooled to room temperature. The solution was filtered through a glass pipette with a pad of cotton and concentrated. Purified by flash chromatography with hexanes/diethyl ether (4 : 1 → 2 : 1 → 1 : 1) to afford **Con-BEP-4** as purple solid (22.5 mg, 26.2 mmol) in 37% yield. $^1$H NMR (500 MHz, $CDCl_3$) $\delta$ 16.52 (s, 1H), 7.57 (s, 1H), 7.29 (d, $J$ = 7.9 Hz, 1H), 7.08 (d, $J$ = 11.8 Hz, 6H), 6.99–6.94 (m, 1H), 6.56 (d, $J$ = 4.3 Hz, 1H), 6.14 (s, 1H), 4.99 (m, 1H), 4.18 (s, 4H), 2.56–2.36 (m, 27H), 1.32 (d, $J$ = 6.0 Hz, 6H). $^{13}$C NMR (126 MHz, $CDCl_3$) $\delta$ 294.3 (from HSQC), 211.7, 159.6, 153.9, 152.1, 145.0, 144.3, 140.5, 139.0, 136.7, 133.9, 129.5, 129.2, 128.4, 125.5, 124.9, 123.8, 123.3, 122.0, 117.9, 114.2, 75.6, 66.0, 37.3, 32.1, 29.9, 22.9, 21.2, 17.0, 16.5, 15.4, 15.2, 14.3. HRMS (APCI+) $m/z$: calculated for $C_{43}H_{49}BF_2N_4ORu$ (M-$Cl_2$ + H$^+$) 789.30837; found 789.30242.

**2-(4-Isopropoxy-3-vinylphenol)-4,4,5,5-tetramethyl-1,3,2-dioxaborolane (3).** 4-Bromo-1-isopropoxy-2-vinylbenzene (203 mg, 0.884 mmol), KOAc (248.5 mg, 2.53 mmol, 3.0 equiv.), Bis(pinacolato) diboron (267.9 mg, 1.05 mmol, 1.25 equiv.), and Pd(dppf)$Cl_2$·$CH_2Cl_2$ (34.5 mg, 0.042 mmol, 0.05 equiv.) were combined in an oven-dried 100 mL 2-neck flask with a magnetic stir-bar and dissolved in 1,4-dioxane (5 mL). The solution was degassed for 20 minutes, and the flask was added to a 75 °C preheated oil bath to stir for 48 hours. After completion, the flask was cooled to room temperature and filtered through a plug of Celite with hexanes and concentrated onto silica. Purified by flash chromatography with hexanes/ethyl acetate to afford the desired product **3** as a white solid (84.1 mg, 0.292 mmol, 35%). $^1$H NMR (500 MHz, $CDCl_3$) $\delta$ 7.92 (s, 1H), 7.66 (d, $J$ = 8.2 Hz, 1H),

7.03 (dd, $J$ = 17.8, 11.2 Hz, 1H), 6.87 (d, $J$ = 8.3 Hz, 1H), 5.82 (d, $J$ = 17.7 Hz, 1H), 5.23 (d, $J$ = 11.1 Hz, 1H), 4.61 (sept, $J$ = 6.1 Hz, 1H), 1.36 (d, $J$ = 6.1 Hz, 6H), 1.34 (s, 12H). $^{13}$C NMR (126 MHz, $CDCl_3$) $\delta$ 157.9, 135.8, 133.8, 132.0, 127.2, 114.5, 112.9, 83.7, 70.5, 25.0, 22.3. HRMS (APCI$^+$) $m/z$: calculated for $C_{17}H_{26}BO_3$ (M + H$^+$) 289.19695; found 289.19514.

**Con-B-5.** To a 250 mL 2-neck round bottom flask containing **1** (164.6 mg, 613 μmol, 1.1 equiv.), **3** (160.6 mg, 557 μmol), $K_2CO_3$ (231.1 mg, 1.67 mmol, 3 equiv.), and Pd(dppf)$Cl_2$·$CH_2Cl_2$ (136.5 mg, 167 μmol, 0.3 equiv.). A nitrogen atmosphere was established and 1,4 dioxane : water (5 : 1) solution was added to the flask *via* syringe and the solution was degassed for 20 minutes. The flask was added to a 100 °C pre-heated oil bath and stirred for 4.5 hours until completion. The solution was extracted with ethyl acetate (3 × 50 mL) and washed with water and brine (3 × 100 mL), dried with sodium sulfate and concentrated under reduced pressure to yield an orange solid. Purification by column chromatography with hexanes/$CH_2Cl_2$ gradient of 40% → 70% to yield **Con-B-5** as an orange solid (34.1 mg, 86.5 μmol, 16%) $^1$H NMR (500 MHz, $CDCl_3$) $\delta$ 7.98 (d, $J$ = 2.4 Hz, 1H), 7.84 (dd, $J$ = 8.7, 2.4 Hz, 1H), 7.19 (d, $J$ = 4.3 Hz, 1H), 7.09 (dd, $J$ = 17.7, 11.1 Hz, 1H), 6.95 (d, $J$ = 8.7 Hz, 1H), 6.56 (d, $J$ = 4.1 Hz, 1H), 6.12 (s, 1H), 5.83 (dd, $J$ = 17.8, 1.6 Hz, 1H), 5.27 (dd, $J$ = 11.1, 1.5Hz, 1H), 4.63 (sept, $J$ = 6.1 Hz, 1H), 2.56 (s, 3H), 2.54 (s, 3H), 2.41 (s, 3H), 1.39 (d, $J$ = 6.1 Hz, 6H). $^{13}$C NMR (126 MHz, $CDCl_3$) $\delta$ 157.6, 156.1, 155.1, 143.1, 140.3, 136.2, 133.2, 131.9, 129.9 (t, $J_{CF}$ = 5.0 Hz), 128.0 (t, $J_{CF}$ = 3.4 Hz), 127.3, 125.5, 125.4, 122.4, 118.1, 114.6, 113.0, 70.7, 29.8, 22.4, 16.8, 16.5, 15.0. HRMS (APCI$^+$) $m/z$: calculated for $C_{23}H_{26}BF_2N_2O$ (M + H$^+$) 395.21008; found 395.20524, $C_{23}H_{25}BF_2N_2ONa$ (M + Na$^+$) 417.19202; found 417.18711.

**Con-BEP-5.** In a $N_2$ filled glovebox, an oven-dried 20 mL Schlenk flask containing **Con-B-5** (28.2 mg, 0.072 mmol, 1.0 equiv.), Grubbs Catalyst M310 (53.6 mg, 0.072 mmol, 1.0 equiv.), and amberlyst 15 resin (60.8 mg, 0.286 mmol, 4.0 equiv.) was suspended in anhydrous $CH_2Cl_2$ (2.5 mL). The flask was placed into a 40 °C preheated oil bath to stir for 1 hour after which time the flask was cooled to room temperature. The solution was filtered through a glass pipette with a pad of cotton and concentrated. Purified by flash chromatography with hexanes/diethyl ether (4 : 1 → 2 : 1 → 1 : 1) to afford **Con-BEP-5** as a red solid (8.9 mg, 0.0104 mmol) in 15% yield. $^1$H NMR (500 MHz, $CDCl_3$) $\delta$ 16.50 (s, 1H), 8.22 (dd, $J$ = 8.6, 2.3 Hz, 1H), 7.34 (d, $J$ = 2.3 Hz, 1H), 7.19 (d, $J$ = 4.0 Hz, 1H), 7.07 (s, 4H), 6.88 (d, $J$ = 8.8 Hz, 1H), 6.43 (d, $J$ = 4.5 Hz, 1H), 6.13 (s, 1H), 4.93 (sept, $J$ = 6.2 Hz, 1H), 4.18 (s, 4H), 2.59 (s, 3H), 2.53 (s, 3H), 2.48 (s, 12H), 2.44 (s, 3H), 2.38 (s, 6H), 1.30 (d, $J$ = 6.1 Hz, 6H). $^{13}$C NMR (126 MHz, $CDCl_3$) $\delta$ 296.8 (from HSQC), 211.6, 158.3, 153.5, 153.0, 145.1, 143.5, 140.5, 139.1, 136.2, 133.4, 130.8, 129.5, 129.2, 128.4, 127.6, 125.3, 123.8, 122.6, 118.1, 112.8, 75.7, 51.6, 37.2, 32.1, 29.8, 29.5, 22.8, 21.3, 21.2, 16.9, 16.5, 14.3. HRMS (APCI$^+$) $m/z$: calculated for $C_{43}H_{50}BF_2N_4ORu$ (M + H$^+$) 789.30837; found 789.30209.

**Photophysical characterization and structure.** Samples for excitation, emission and absorption measurements were contained in 1 cm × 1 cm cuvette (Special optical glass (SOG) – Starna). Fluorescence spectra were obtained using a Cary Eclipse Fluorimeter (Varian). Emission spectra were collected with excitation at 505 nm. Excitation spectra were collected observing at 580 or 630 nm. Absorbance spectra were acquired using a Cary Bio100 UV spectrophotometer (Varian). Absorbance spectra were collected in dual beam mode with zero and baseline correction. The absorbance was kept below 0.1 to minimize reabsorption.

**Determination of molar absorptivity.** Absorption spectra were collected for the samples over a range of concentrations (0.0–1.7 μM) maintaining absorption values below 0.1 (Fig. S1 and S2, ESI†). Absorption spectra were collected from 700–440 nm with zero and baseline corrections. The molar absorption coefficient ($\varepsilon$) was determined from the slope of absorbance at $\lambda_{max}$ *vs.* concentration (Fig. S3 and S4, ESI†).

**Determination of relative quantum yields.** Relative quantum yields were determined by comparison to rhodamine 6G ($\Phi$ = 0.95) as a standard in EtOH ($\eta$ = 1.36).[1] **Con-B-4**, **Con-B-5**, **Con-BEP-4**, and **Con-BEP-5** were measured in toluene ($\eta$ = 1.4969). Absorption and emission spectra were collected for the standard and sample over a range of concentrations (0.0–1.7 μM) maintaining absorption values below 0.1. Absorption spectra were collected from 700–440 nm with zero and baseline corrections. A linear correlation between concentration and absorption was confirmed over the range of concentrations used. Fluorescence was monitored to collect the full emission spectra to the extent possible exciting samples at 505 nm observing from 520–700 nm. Each sample or standard integrated emission was plotted as a function of absorbance at the excitation wavelengths (505 nm), which provided excellent linear fits for all samples (Fig. S5–S7, ESI†). The slope for each sample was determined in at least two different experiments and the average slope was used for comparison to the standard.

**Calculations.** DFT calculations were carried out in Gaussian using the b3lyp/6-311+G(d) basis set. Molecular orbital maps were determined on energy minimized structures with and without restrictions to the dihedral angle between the pyrrole and chelating ligand moieties (Fig. S8–S12, ESI†).

### Response to ethylene

**Ethylene gas.** The overall response of each probe to ethylene was determined by exposing solutions of probe in toluene to a balloon of ethylene gas and monitoring emission intensity over time. Solutions were prepared in septum capped cuvettes by dilution of standard aliquots (1 mM) in toluene to provide an initial [**Con-BEP-4**] = 2 μM and [**Con-BEP-5**] = 2 μM. A $t$ = 0 measurement was acquired and then the solution was exposed to an excess of ethylene by flushing the headspace of the cuvette with ethylene until no mixing lines could be observed indicating that the solution was saturated with ethylene. During the initial dissolution of ethylene into toluene the solution was mixed by vortexing to enhance the rate of ethylene dissolution and achieve a homogenous solution. Fluorescence spectra were collected at regular intervals exciting at 505 nm and observing from 520–700 nm. Data were normalized to the $t$ = 0 timepoints.

**Ethephon in PBS.** A solution of 2.5 mL of ethephon (24 mmol) in 40% aqueous solution was added to 7 mL PBS

buffer (dPBS 1X, Caisson Labs) to a 100 mL round bottom flask containing a magnetic stir bar. A 1 M solution of NaOH (18 mL) was used to adjust the pH to 7.0. **Con-BEP-4** (12 mg, 0.014 mmol, 1 equiv.) was dissolved in 20 mL of toluene added to the flask. The biphasic solution was vigorously stirred at 37 °C overnight with samples assessed for fluorescence increase at regular intervals. After 22 h, the solution was extracted with toluene (3 × 15 mL) and concentrated to provide an orange solid. Crude $^1$H NMR indicated no remaining **Con-BEP-4** and signals readily associated with **Con-B-4** (Fig. S18, ESI†). The crude mixture was purified by flash chromatography using 1 : 1 hexanes/ethyl acetate to provide orange crystals of **Con-B-4** in approximately quantitative yield.

**Ethephon in DMEM.** A solution of **Con-BEP-4** in PhMe (20 μM, 10 mL) was stirred under biphasic conditions with cell growth media (DMEM supplemented with 10% fetal bovine serum and 1% penicillin–streptomycin) with or without added ethephon (100 μL, titrated to back to neutral pH). The biphasic mixtures were vigorously stirred at 37 °C with samples assessed for fluorescence increase at regular intervals (Fig. S19, ESI†).

### Live cell imaging studies

A549 cells were cultured in Dulbecco's Modified Eagle Medium supplemented with 10% fetal bovine serum and 1% penicillin–streptomycin in LabTek 8-well dishes (400 μL per well). At approximately 80% confluency cells were 0, 1, or 2 μL treated with 40% aqueous solution of ethephon (AK Scientific) and the media was immediately titrated with a 1 M NaOH solution back to neutral pH as indicated by the phenol red in DMEM (~7–10 μL 1 M NaOH per μL ethephon solution). The cells were incubated for 1–3 h at 37 °C in 5% $CO_2$. After the defined period of DMEM (or DMEM + Ethephon) solutions were removed, cells were washed with pre-warmed PBS (1 × 400 μL), and then stained with **Con-BEP-4** in prewarmed PBS (1 μM, 0.5% DMSO). The cells were again incubated for 30–60 min at 37 °C in 5% $CO_2$, then removed for imaging. Control cells were treated in the same fashion, except no ethephon was added. Confocal images of A549 cell were acquired on a Flowview 3000 microscope with a 60× objective using the FV315-SW confocal control software. **Con-BEP-4** (or the resulting ethylene adduct – **Con-B-4**) were excited using either a 488 nm laser (2% Laser power, HV 500, Gain 2×, offset 3%, observe 578–602 nm) or a 561 nm laser (3% Laser power, HV 550, Gain 2×, offset 3%, 539–601 nm). DIC images were obtained with the 640 nm laser. At least three representative fields of cells within the same well were imaged. Image analysis and quantification was performed using ImageJ (National Institutes of Health) with the OlympusViewer plugin. The threshold was appropriately adjusted to the same level for all images being compared and mean fluorescence intensity was measured across the entire field using the measure function.

### Cytotoxicity assay

A549 cells were cultured in DMEM supplemented with 10% fetal bovine serum and 1% penicillin–streptomycin in 96-well plates (~$10^4$ cells per well). Cell culture media was removed, and cells were treated with **Con-BEP-4**, **Con-B-4**, **Con-BEP-5**, or **Con-B-5** (0.2–2 μM) dissolved in Opti-MEM (1X) with 0.5% DMSO (100 μL per well) for 1 hour. After incubation the wells were aspirated, and fresh Opti-MEM was added to the wells with 10 μL of MTT reagent in PBS and incubated for 3 hours. After incubation the wells were aspirated and 100 μL of DMSO was added to the wells. Absorbance readings at 570 nm were measured on a plate reader (Tecan Infinite M200 Pro). The normalized absorbance was averaged over a minimum of four replicates for each condition evaluated (Fig. S21, ESI†).

## Author contributions

NJD, NBW, and BWM designed and performed experiments. NJD and BWM analysed data and wrote the manuscript. BWM conceived and supervised the research.

## Conflicts of interest

There are no conflicts to declare.

## Acknowledgements

Prof. Andrei G. Kutateladze (University of Denver) is acknowledged for assistance with computational work. Tyler D. Ball and Prof. Sunil Kumar (University of Denver) are acknowledged for assistance with cytotoxicity assays. Prof. Todd A. Wells (University of Denver) is thanked for helpful discussions. This material is based upon work supported by the National Science Foundation under Grant CHE-1900482. Research reported in this publication was supported by NIGMS R35GM150937.

## References

1 J. J. Kieber, *Annu. Rev. Plant Physiol. Plant Mol. Biol.*, 1997, **48**, 277–296.
2 K. L. C. Wang, H. Li and J. R. Ecker, *Plant Cell*, 2002, **14**, S131–S151.
3 J. M. Alonso and A. N. Stepanova, *Science*, 2004, **306**, 1513–1515.
4 S. Janssen, K. Schmitt, M. Blanke, M. L. Bauersfeld, J. Wollenstein and W. Lang, *Philos. Trans. R. Soc., A*, 2014, **372**, 20130311.
5 F. Caprioli and L. Quercia, *Sens. Actuators, B*, 2014, **203**, 187–196.
6 K. M. Light, J. A. Wisniewski, W. A. Vinyard and M. T. Kieber-Emmons, *JBIC, J. Biol. Inorg. Chem.*, 2016, **21**, 715–728.
7 E. E. Dumelin and A. L. Tappel, *Lipids*, 1977, **12**, 894.
8 L. M. Paardekooper, G. van den Bogaart, M. Kox, I. Dingjan, A. H. Neerincx, M. B. Bendix, M. ter Beest, F. J. M. Harren, T. Risby, P. Pickkers, N. Marczin and S. M. Cristescu, *Sci. Rep.*, 2017, **7**, 6889.
9 K. H. Jensen and B. W. Michel, *Analysis Sensing*, 2023, **3**, e202200058.
10 X. Yang, Q. Zhang, S. Zhang, M. Lai, X. Ji, Y. Ye, H. Li and M. Zhao, *Coord. Chem. Rev.*, 2023, **487**, 215154.
11 J. Chatt, L. A. Duncanson and L. M. Venanzi, *J. Chem. Soc.*, 1955, 4456–4460.

12 O. Green, N. A. Smith, A. B. Ellis and J. N. Burstyn, *J. Am. Chem. Soc.*, 2004, **126**, 5952–5953.
13 M. Santiago Cintrón, O. Green and J. N. Burstyn, *Inorg. Chem.*, 2012, **51**, 2737–2746.
14 B. Esser and T. M. Swager, *Angew. Chem., Int. Ed.*, 2010, **49**, 8872–8875, S8872/1-S8872/15.
15 B. Esser, J. M. Schnorr and T. M. Swager, *Angew. Chem., Int. Ed.*, 2012, **51**, 5752–5756, S5752/1-S5752/13.
16 Y. Hitomi, T. Nagai and M. Kodera, *Chem. Commun.*, 2012, **48**, 10392–10394.
17 P. Cabanillas-Galan, L. Farmer, T. Hagan, M. Nieuwenhuyzen, S. L. James and M. C. Lagunas, *Inorg. Chem.*, 2008, **47**, 9035–9041.
18 S. N. W. Toussaint, R. T. Calkins, S. Lee and B. W. Michel, *J. Am. Chem. Soc.*, 2018, **140**, 13151–13155.
19 M. Sun, X. Yang, Y. Zhang, S. Wang, M. W. Wong, R. Ni and D. Huang, *J. Agric. Food Chem.*, 2019, **67**, 507–513.
20 K. Vong, S. Eda, Y. Kadota, I. Nasibullin, T. Wakatake, S. Yokoshima, K. Shirasu and K. Tanaka, *Nat. Commun.*, 2019, **10**, 5746.
21 D. Fong, S.-X. Luo, R. S. Andre and T. M. Swager, *ACS Cent. Sci.*, 2020, **6**, 507–512.
22 M. Wu, C. Yin, L. Fu, T. Liu, M. Jiang, Q. Sun, L. Chen and N. Niu, *Chem. Eng. J.*, 2022, **435**, 135045.
23 Y. Chen, W. Yan, D. Guo, Y. Li, J. Li, H. Liu, L. Wei, N. Yu, B. Wang, Y. Zheng, M. Jing, J. Zhao and Y. Ye, *Angew. Chem., Int. Ed.*, 2021, **60**, 21934–21942.
24 Y. Yang, H. Bian, Z. Jia and P. Tu, *ACS Omega*, 2023, **8**, 15350–15359.
25 J. Ohata, K. J. Bruemmer and C. J. Chang, *Acc. Chem. Res.*, 2019, **52**, 2841–2848.
26 K. J. Bruemmer, S. W. M. Crossley and C. J. Chang, *Angew. Chem., Int. Ed.*, 2020, **59**, 13734–13762.
27 M. H. Lim, B. A. Wong, W. H. Pitcock, D. Mokshagundam, M.-H. Baik and S. J. Lippard, *J. Am. Chem. Soc.*, 2006, **128**, 14364–14373.
28 M. H. Lim, D. Xu and S. J. Lippard, *Nat. Chem. Biol.*, 2006, **2**, 375–380.
29 B. W. Michel, A. R. Lippert and C. J. Chang, *J. Am. Chem. Soc.*, 2012, **134**, 15668–15671.
30 M. Strianese and C. Pellecchia, *Coord. Chem. Rev.*, 2016, **318**, 16–28.
31 D. A. Iovan, S. Jia and C. J. Chang, *Inorg. Chem.*, 2019, **58**(20), 13546–13560.
32 B. J. Bezner, L. S. Ryan and A. R. Lippert, *Anal. Chem.*, 2020, **92**, 309–326.
33 J. Alday, A. Mazzeo and S. Suarez, *Inorg. Chim. Acta*, 2020, **510**, 119696.
34 R. R. Walvoord, M. R. Schneider and B. W. Michel, in *Carbon Monoxide in Drug Discovery: Basics, Pharmacology, and Therapeutic Potential*, ed. B. Wang and O. Wang, John Wiley & Sons, Hoboken, NJ, 2022, pp. 321–344.
35 X. Yang, Z. Yuan, W. Lu, C. Yang, M. Wang, R. Tripathi, Z. Fultz, C. Tan and B. Wang, *J. Am. Chem. Soc.*, 2023, **145**, 78–88.
36 D. F. Sauer, T. Himiyama, K. Tachikawa, K. Fukumoto, A. Onoda, E. Mizohata, T. Inoue, M. Bocola, U. Schwaneberg, T. Hayashi and J. Okuda, *ACS Catal.*, 2015, **5**, 7519–7522.
37 J. Morstein, D. Höfler, K. Ueno, J. W. Jurss, R. R. Walvoord, K. J. Bruemmer, S. P. Rezgui, T. F. Brewer, M. Saitoe, B. W. Michel and C. J. Chang, *J. Am. Chem. Soc.*, 2020, **142**, 15917–15930.
38 V. Leen, E. Braeken, K. Luckermans, C. Jackers, M. V. der Auweraer, N. Boens and W. Dehaen, *Chem. Commun.*, 2009, 4515–4517.
39 S. Monsaert, R. Drozdzak, V. Dragutan, I. Dragutan and F. Verpoort, *Eur. J. Inorg. Chem.*, 2008, 432–440.
40 C. A. Urbina-Blanco, A. Leitgeb, C. Slugovc, X. Bantreil, H. Clavier, A. M. Z. Slawin and S. P. Nolan, *Chem. – Eur. J.*, 2011, **17**, 5045–5053.